

Article

Reversible Switching of Icing Properties on Pyroelectric Polyvinylidene Fluoride Thin Film Coatings

Dirk Spitzner *, Ute Bergmann *, Sabine Apelt, Richard A. Boucher and Hans-Peter Wiesmann

Institute of Materials Science, Technische Universität Dresden, Helmholtzstr. 7, Dresden 01069, Germany; E-Mails: Sabine.Apelt@tu-dresden.de (S.A.); Richard.Boucher@tu-dresden.de (R.A.B.); Hans-Peter.Wiesmann@tu-dresden.de (H.-P.W.)

* Authors to whom correspondence should be addressed; E-Mails: Dirk.Spitzner@tu-dresden.de (D.S.); Ute.Bergmann@tu-dresden.de (U.B.); Tel.: +49-351-463-34504 (D.S.); +49-351-463-33895 (U.B.); Fax: +49-351-463-33207 (D.S. & U.B.).

Academic Editor: D. K. Sarkar

Received: 28 August 2015 / Accepted: 14 October 2015 / Published: 20 October 2015

Abstract: In this work a new approach for ice repellent coatings is presented. It was shown that the coatings cause a decrease or increase in the freezing temperature of water depending on the alignment of an external electric field. For this coating the commonly used pyroelectric polymer polyvinylidene fluoride was deposited as a thin film on glass. The samples were dip-coated and subsequently thermally-treated at 140 °C for 1 h. All samples were found to cause a reduction of the icing temperature of water on their surface in comparison to uncoated glass. On several samples an external electric field was applied during this thermal treatment. The field application was found to cause a remarkable reduction of the icing temperature where a maximum lowering of the freezing temperature of 3 K compared to uncoated glass could be achieved. The actual achieved reduction of the icing temperature was observed to depend on the polarity of the field applied during the thermal treatment. Furthermore, a repetition of the thermal treatment under oppositely directed electric fields led to a switchable freezing behavior of water according to the direction of the applied field. With an increasing number of cycles of switching of the icing property a slight training effect towards lower freezing temperatures was observed.

Keywords: anti-icing; coatings; defrost; electric field; freezing; ice adhesion; icephobic surfaces; pyroelectric; super-hydrophobicity; roughness

1. Introduction

Icing phenomena are an issue affecting the reliability of objects in everyday life such as power lines, wind generators, and leading edges of airplane wings. Frost formation reduces the efficiency of solar panels in addition to the effects of less sunshine during the cold times of the year. Ice formation also causes damage in porous structures, such as mortar and concrete, since the specific volume increases with decreasing temperature.

The strategies used so far for ice-free surfaces can be divided into two approaches: reducing the adhesion force between ice and the material, and reducing the freezing temperature by restricting the heterogeneous nucleation. One approach to ice repellent surface coatings is the application of superhydrophobic coatings, since a small contact area should lead to less adhesion of ice [1]. As bonded and broken hydrogen bonds play an important role inside liquid water and, hence, for ice formation [2], Petrenko and Peng systematically investigated ice adhesion on self-assembling monolayers and correlated the shear strength with the degree of hydrogen bonding and, hence, the contact angle [3]. Porous materials such as TiO₂-SiO₂ mixed layers [4] can be used to cause a given volume to adhere to the solid, since the freezing process depends on the interaction of the initial volume of freezing water and provided cavities in a porous surface shell [5]. A wide range of structured hydrophobic surfaces have been proposed and investigated, including RF-sputtered surfaces [6,7]. Sol-gel derived coatings could also be used since a wide range of properties can be set by varying the precursors and production parameters during the preparation of the sol-gel layers [8]. However, with respect to the suppression of ice adhesion hydrophobic and superhydrophobic surfaces have been only partially successful because the required structures for superhydrophobicity run the risk of being damaged in icing-deicing processes. Moreover, wetting properties strongly depend on the environmental conditions such as humidity and may switch from a Cassie-Baxter-state with air trapped beneath the droplets to a Wenzel-state with water in full contact with the surface over its' complete morphology [9,10]. Furthermore, these hydrophobic and icephobic phenomena are based on different mechanisms characterized by different typical length scales [11]. Under certain environmental conditions hydrophilicity can enhance icephobic properties as shown by Jung *et al.* [12].

Nature derived biomimetic approaches such as anti-freeze-proteins and bacteria (ice nucleating matter) can increase the freezing temperature and thus extend the freezing time as well as inhibit Ostwald ripening of crystallites [13–16]. The direct implementation of these approaches has its limitation in technical design since proteins might denature or they might be a food source for microorganisms provoking fouling processes. However, there exists a variety of biomimetic adaptations of hydrophobic-hydrophilic nanoscopic clusters on technical materials. Another appropriate approach represents switchable hydrophobic-hydrophilic and swellable surfaces working as a sponge-like liquid reservoir [17–19]. Combined inflexible and flexible layers based on oil trapped in silicon structures have at present a limited number of operational cycles due to oil depletion or water penetration into the substrate [20] and have limited application due to the risk of frost damage in a similar manner to the porous structures mentioned above.

Some ice repellent routes, such as the heating of land lines by a wire-in-wire approach [21] work with an external energy input. By using piezo actuators which distort the workpiece and, hence, shear off ice droplets the energy consumption can be reduced significantly [22]. The distortion, however, still requires external control and causes an additional strain which the material has to bear.

A further approach that has been used to affect the icing process is the utilization of electric fields in order to influence the crystallization process of the polar water molecules. According to Petrenko *et al.*, this leads to a higher adherence to surfaces and a stronger binding of ice [23]. Petersen *et al.* even investigated the stimulation of ice formation by pulsed electric fields [24].

Ehre *et al.* reported different crystallization behavior on different sides of pyroelectric single crystals, which exhibit surface charges in the case of a temperature change. It could be shown, that differently-charged surfaces lead to different ice crystallization behaviors starting from the solid-liquid interface (for the case of positively charged solid surface) or liquid-gaseous interface (for the case of negatively charged solid surface) [25]. As a consequence the crystallization on a negatively charged surface is suppressed in comparison to a similar positively charged surface. Pyroelectric response is a possible response of dielectric materials with oriented dipoles towards temperature change and the pyroelectric effect is observed on ceramic [26] as well as polymeric materials [27]. A widely-used pyroelectric polymer is polyvinylidene fluoride. A pyroelectric behavior can be observed in the case of equally oriented monomers in the carbon chain, in the so called trans-gauche-conformation. In this case an equilateral orientation of all hydrogen atoms along on one side and fluorine atoms of the opposite side of the c-chain is observed. This material state can be achieved by different preparation routes such as mechanical stretching, thermal treatment or the addition of co-polymers.

In the present work for the first time a pyroelectric material is used as an icephobic coating. In this layer the intrinsic properties lead to an active response to temperature changes which influence the electrochemical interaction of the water molecules and the solid surface. In the freezing process temperature changes can be induced with different signs. Cooling can be caused by changes of the environmental conditions (temperature drop) alternatively a local temperature increase can be caused by a heat input during the freezing process (crystallization energy). Hence the material's reaction during the freezing process and its intended icephobic property are at the same time an intrinsic property of the material itself and neither needs external energy input nor external control mechanisms. Certain polymers have been suggested by others to be economically priced ice repellent coatings, which can be used in large-scale-production. With regard to renewable energy pyroelectrics, polymers in general as well as the investigations the polyvinylidene fluoride/trifluorethylene copolymer (P(VDF-TrFE)) have been suggested in particular to be a good material for energy harvesting from waste heat [28,29] by means of the Olsen cycle [30].

2. Experimental Section

2.1. Materials and Preparation

For these investigations P(VDF-TrFE) was used. It contains a fraction of the pyroelectric β -phase after growing from solution due to the copolymerization. Glass substrates ($20 \times 30 \text{ mm}^2$, thickness 0.5 mm, purchased from Crystec GmbH), were dip-coated with P(VDF-TrFE) in a cyclohexanone solvent

(solvene™, purchased from Solvay-Solexis) at a withdrawal speed of 1.2 mm/s. Each sample was coated five times with a drying pause of 20 min in ambient conditions between two coating sequences in order to achieve a usable film thickness. Subsequently, a thermal treatment at 140 °C in a pre-heated furnace for 1 h was applied. In order to align the dipoles of the pyroelectric coating, the samples were clamped on a metal plate which worked as a counter electrode of a capacitor arrangement (see Figure 1), with a distance between electrodes of 1.4 mm. A voltage of ± 4 kV was applied across the electrodes. The electrode at high potential was covered with a Kapton foil for insulation purposes. After 1 h of thermal treatment the electric field was switched off (in the case of applied fields), samples were subsequently taken out of the oven and cooled down in ambient conditions to room temperature. Additional thermal treatments were carried out after the measurement of the freezing temperature in order to recognize changes in the same samples with respect to icing properties.

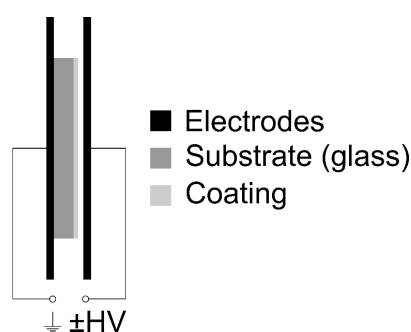


Figure 1. Sketch of setup to polarize the samples.

2.2. Optical Microscopy

The surface morphology was characterized by means of optical microscopy using polarized light and a $\lambda/4$ plate in reflected-light mode.

2.3. Measurement

In order to determine the icing temperature, samples were loaded into a cooling chamber (LTS 350, Linkam Scientific Instruments Ltd, Surrey, UK) as shown in Figure 2.

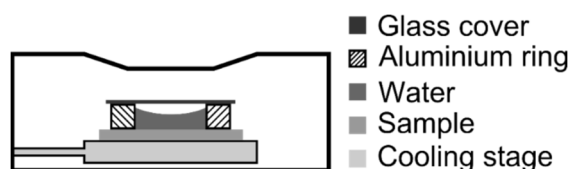


Figure 2. Sketch of cooling-setup (cross section), the neck on top of the cooling stage contains a window facilitating the visual observation of any ice formation.

For freezing point measurements an aluminum ring (5 mm outer diameter, 3 mm inner diameter) was placed onto the sample in order to form a reservoir and a 10 μ L-drop of de-ionized water was put inside the ring directly onto the surface of the sample. The water reservoir was covered by a glass slide in order to prevent evaporation during the cooling process due to the chamber being flushed by cold nitrogen from a liquid nitrogen reservoir.

In the first step of the measurement process the stage was cooled down to 5 °C and kept at this temperature for 10 min in order to achieve a thermal equilibrium state of the setup in particular of the pyroelectrics, their surface and screening charges. Afterwards, the whole setup was cooled down at a cooling rate of 1 K/min until the water froze. The measurement stage was, subsequently, reheated to 5 °C again and the process was repeated. Up to five freezing/defrosting cycles were completed; the freezing measurements were made for at least three different water droplets in order to exclude effects of preparation. Hence, at least 15 freezing temperatures were measured for each prepared state. The droplet was observed by using a microscope and the temperature of the measurement stage measured in order to recognize the point of freezing.

3. Results

3.1. Surface Characterization

The dip-coated P(VDF-TrFE)-coatings have a non-negligible surface roughness. Surface roughness is especially important in context of superhydrophobicity and the samples particular icing characteristics. The structure appears to be scarred, where the ridge/valley width is up to 3 µm. The mean roughness R_a of these surfaces, measured by confocal white light microscopy (μ -surf) is 0.070 µm. The appearance of the surface morphology in reflected-light-microscopy is shown in Figure 3 of the same sample.

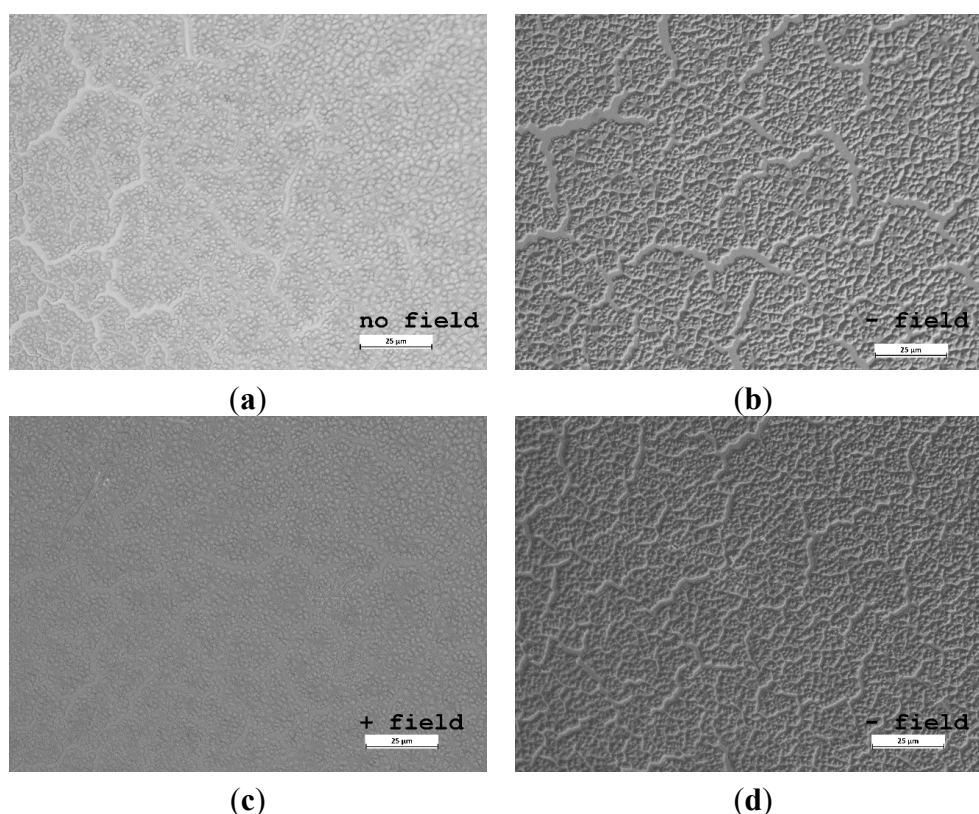


Figure 3. Optical reflected-light microscopy of a P(VDF-TrFE)-coated glass sample after thermal treatment at 140 °C (length of scale bar: 25 µm); (a) with no electric field applied; (b) whilst negative electric field was applied; (c) after further positive electric field was applied; and (d) after successive negative electric field was applied.

In this figure, a compilation of surface micrographs taken after different thermal treatments is shown. The polymer film exhibits a specific pattern which is dependent on the thermal treatment. It is suggested that this is influenced by crystalline and amorphous areas. Independent of whether an electric field is applied or not, the typical structure length stays the same; however, by applying no field or a positively oriented electric field during the thermal treatment convex-like structures appear, whereas a negative electric field seems to induce concave-like structures. Consequently, it would appear that this structure pattern is switchable.

In order to exclude the influence of structure differences on the determined icing temperatures, for the negatively and positively polarized samples, a surface scan by means of confocal white light microscopy (μ -surf) was done. It could be shown, that for either polarization of the sample in the electric field the structure length as well as the structure pattern remained and no structure change occurred as a result of an inversion of the polarity, as seen in Figure 4.

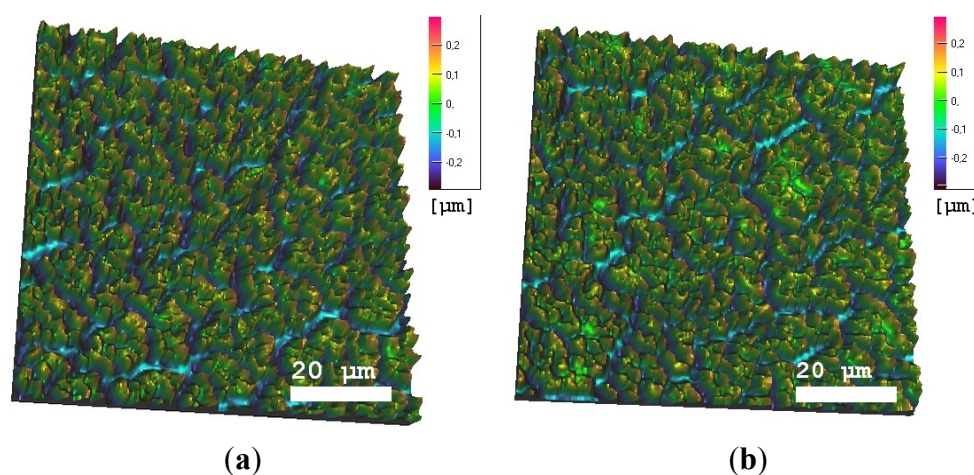


Figure 4. Confocal white-light microscopy of P(VDF-TrFE)-coated glass samples after thermal treatment at 140 °C, illustration of surface roughness; **(a)** with negative electric field applied during thermal treatment; and **(b)** positive electric field applied during thermal treatment of the same sample.

3.2. Freezing Experiments

Figures 5–8 show the freezing temperatures of uncoated and coated surfaces as well as polarized and repeatedly differently polarized coatings. In these figures freezing temperatures are shown in Celsius as this was measured in the experiments. The freezing temperature strongly depends on the particular measurement conditions and, therefore, all discussions make reference to an uncoated glass substrate also tested using the same conditions. The differences in the freezing temperatures compared to the uncoated glass are given in Kelvin. In Figure 5, an annealed (140 °C) P(VDF-TrFE) coating and an uncoated glass reference are compared. As seen in Figure 5, the P(VDF-TrFE)-coating reduces the icing temperature by 1.5 K in comparison to the uncoated glass.

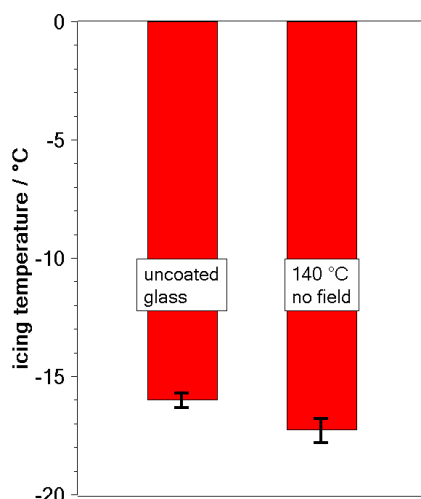


Figure 5. Freezing temperature on P(VDF-TrFE)-coated glass after a thermal treatment at 140 °C with no electric field applied. A comparison is made to uncoated glass.

A further reduction of the freezing temperature, 3 K in total compared to the reference, was achieved by using a further thermal treatment and simultaneously applying a negatively oriented field (Figure 6).

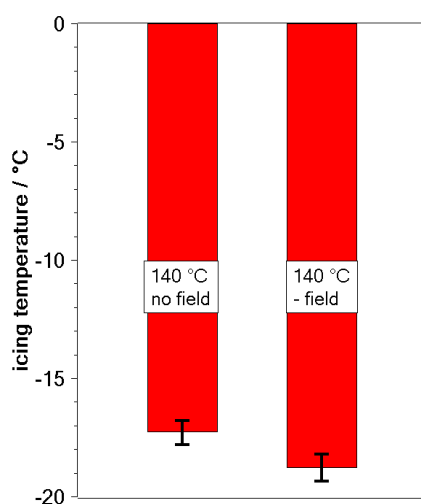


Figure 6. Comparison of the freezing temperature on P(VDF-TrFE)-coated glass after thermal treatments of the same sample at 140 °C for the cases with no electric field applied and with a negative electric field applied.

Figure 7 shows two effects: (a) Applying a positive electric field during the thermal treatment yields a freezing temperature close to the one of the unpolarized state; and (b) the coatings can be re-polarized which allows a switching of the icing properties. The freezing temperature-polarity-correlation was reproducible within the accuracy of the measurement (0.1 K instrumental error + 2σ – statistical error of mean value). The tendency of suppression of the crystallization by negative surface polarization is also confirmed for the case of a sample with a polarization orientation during the first thermal treatment. Due to the repetition of the thermal treatments with alternating directions of the electric field a slight training

effect can be seen since the freezing temperature stays the same to the accuracy of the measurements but the mean value decreases (Figures 7 and 8).

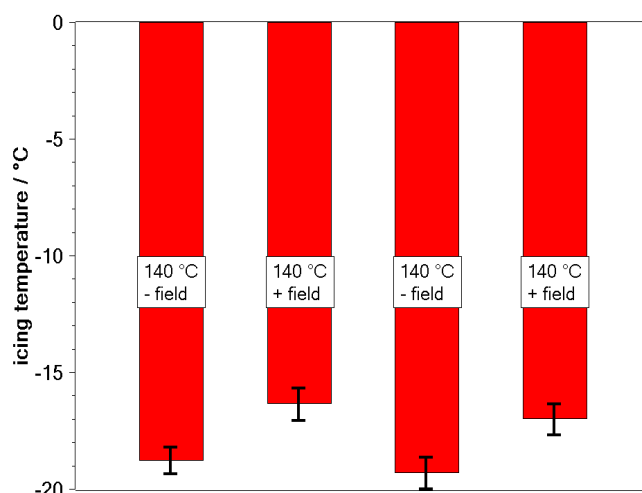


Figure 7. Reversibly-tunable freezing temperature on P(VDF-TrFE)-coated glass after several thermal treatment cycles at 140 °C with an alternating direction of the electric field starting with a negative field orientation subsequent to a no-field-treatment.

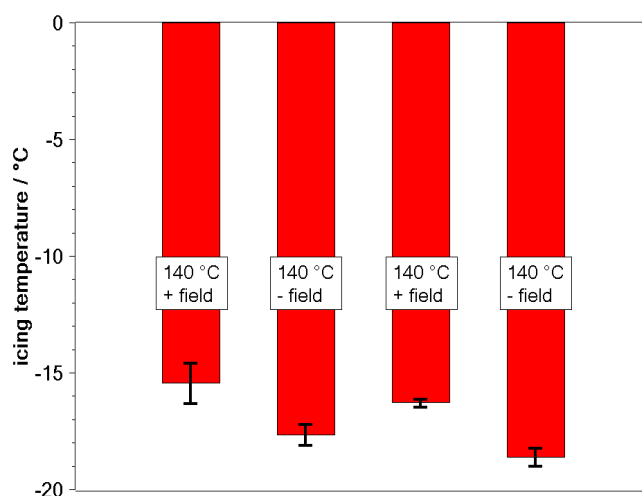


Figure 8. Reversibly-tunable freezing temperature on P(VDF-TrFE)-coated glass after several thermal treatment cycles at 140 °C with alternating direction of the electric field starting with a positive field orientation.

Both the measured freezing temperatures as well as the snap-shots of surface morphology confirm a reversible switchability of the characteristics of P(VDF-TrFE) films. A combination of the microscopy and freezing is shown in Figure 9. In this figure visually observed changes are induced by the presence and the orientation of an electric field during a thermal treatment.

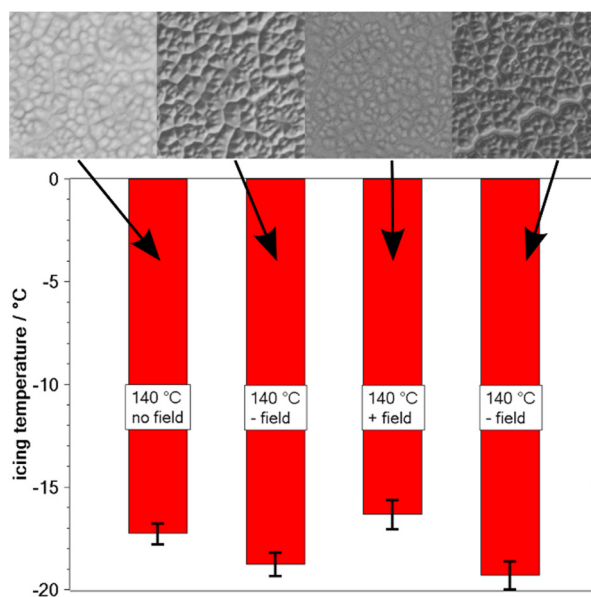


Figure 9. Correlation between electric field direction during thermal treatment, freezing temperature, and surface appearance under light microscopy.

4. Discussion

Due to the change in the icing temperature caused indirectly by the application of an electric field an interaction with the P(VDF-TrFE) structure can be implied. The process might be described by a model in which a pyroelectric exhibits a polarization and a surface charge in accordance with its orientation in a capacitor arrangement according to the applied field direction. However, such a model cannot fully explain the present situation since the polymer material is only partially crystalline and/or pyroelectric. As a consequence, the pyroelectric active regions might be on the surface or inside a non-pyroelectric matrix.

Instead, a model is proposed in which the polarization of pyroelectric parts or particles within a matrix and screening charges are considered, as seen in Figure 10. These pyroelectric regions are immobilized within a matrix in a way that their location is fixed but they still can rotate in order to align in accordance with an external field. The polarization of pyroelectric regions leads to surface charges on the regions. In the equilibrium state these surface charges are compensated by screening charges from the environment (Figure 10a) in order to reduce the free energy of the field caused by these surface charges. During a heating process the temperature change causes a change of the absolute value of the permanent polarization and hence it causes a change of these surface charges in accordance with the pyroelectric effect (Figure 10b). For a period of time after the temperature change surface- and screening charges are not in equilibrium due to the inertia of the system. A net dipole remains and can be orientated along the flux lines due to their interaction with the external electric field (Figure 10c) until the equilibrium state is again achieved. In the equilibrium state pyroelectrics are now aligned and surface charges are compensated by screening charges and, consequently, no net dipole remains (Figure 10d). A subsequent cooling process with no field applied will lead to a change of the value of polarization. This leads again to an appearance of screening charges with the opposite sign in comparison with the charges observed during the heating process. In this case the surface exhibits a net charge of the same polarity as the

electrode which faced the surface during the heat treatment (Figure 10e). This model also works for pyroelectrics with negative pyroelectric coefficients.

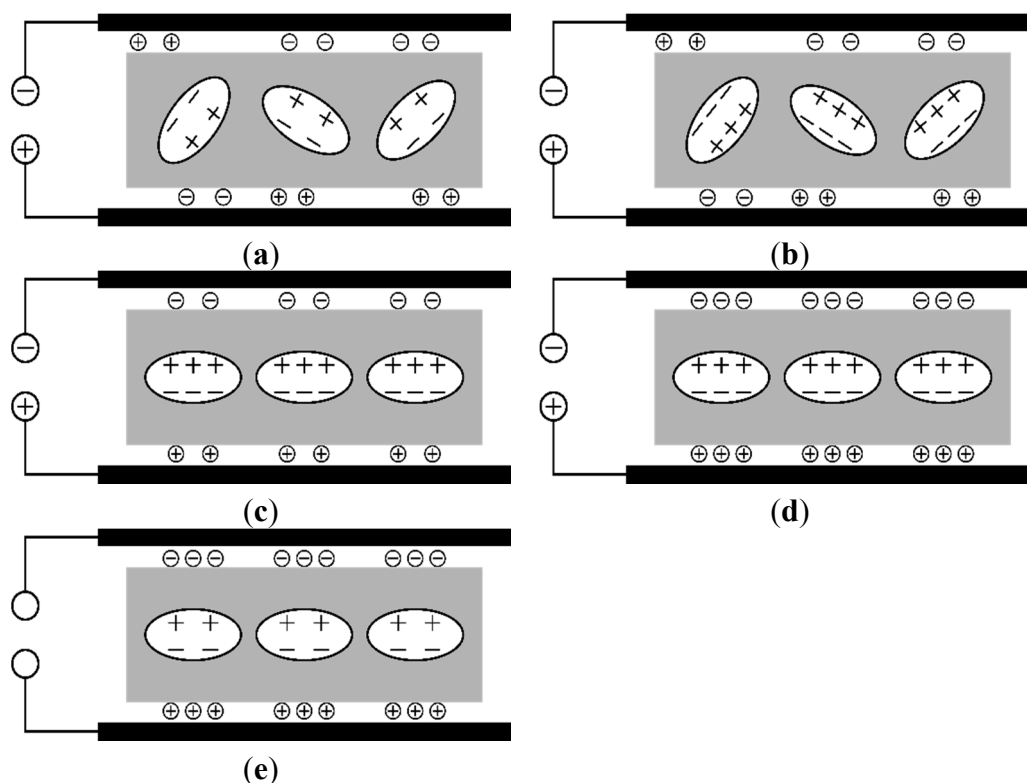


Figure 10. Alignment of P(VDF-TrFE)-clusters in an electric field; (a) surface charges of pyroelectrics (ellipses) and screening charges (circles) in equilibrium state; (b) temperature change induces changes of the polarization and net dipoles will remain; (c) net dipoles are aligned with the field; (d) in the case of no further temperature change, screening charges again fully compensate the pyroelectrically induced surface charges; and (e) cooling process with no field applied evokes a net surface charge related to the polarity of the electrode the surface faced during the polarization process.

A consequence of this process is that a surface, exhibiting a positive net charge during the heating phase, will exhibit a negative net charge during any subsequent cooling process as described above and, hence, lead to higher possible undercooling. The results obtained in this work are in agreement with the observations of Ehre *et al.* In detail, the P(VDF-TrFE) layer can be orientated in a pyroelectric trans-gauche-transformation. This orientation and the freezing temperature respectively, seems to be switchable. The observed switchable freezing temperature is in contradiction to the long standing point of view, that electric fields do not necessarily support the freezing process or will increase the freezing temperature. In contrast to the method presented here the water system in previously-described investigations [20] was cooled down to a supercooled state and an electric field was applied to this supercooled water system or alternatively water was cooled down in the presence of an external field [21]. In this work, however, the establishment of an electric field is part of the cooling process and takes place at the same time as the crystallization process. Moreover, the compensation of charge differences will be effected only in the small band of electro-chemical double layer. This layer is the immediate contact

of secondary crystal seeds to their required external surface. Consequently it provides a very effective way to interrupt the necessary crystal nucleation by charging polarizations and, therefore, to diminish the icing temperature.

Remarkably, the electric field, applied during the thermal treatment, affects the properties of the P(VDF-TrFE) coating although it is heated up to 140 °C. This temperature is above its Curie temperature and, in addition, the electric field was switched off at this temperature. When the electric field is applied to the pyroelectric above its Curie temperature, thus it would be expected that it not could align pyroelectric clusters. However, as reported by Nordheim *et al.* [31] a remanent non-switchable polarization was measured even after heating P(VDF-TrFE) above the Curie temperature.

In this work, the P(VDF-TrFE)-films were influenced by the applied electric fields above the material's Curie temperature, which should be investigated in detail in particular with respect to optimization of ordered films. Aside from this effect, the suspicion of appreciable morphology changes as a result of field polarization could be excluded, such changes would be expected to influence the freezing temperature.

5. Summary/Outlook

In the present work pyroelectric polymer thin films were prepared by dip-coating in order to create ice repellent coatings. The strength of the ice repellency could be increased by the coating's polarization, *i.e.*, orientation of the electric dipoles of the pyroelectric material. This resulted in a switchable icing temperature of the coating in accordance with the polarity of the field. An electric field was applied during the thermal treatment above the Curie temperature of the polyvinylidene trifluorethylene copolymer. With an increasing number of cycles of the thermal treatment and application of the electric field a slight training effect was visible.

It is expected that an increased effect should be achieved by poling the whole coating without thermal treatment in an external electric field above the critical field of approximately 20 MV/m. To explore the interactions between exhibited surface charges of the pyroelectrics and the organization of an electrochemical double-layer in the surrounding fluid further concerted efforts combining icing tests and electrochemical investigations are needed. Furthermore, icing properties should be investigated with regard to frost phenomena which are expected to be more comparable to normal environmental conditions compared to water droplets.

Acknowledgments

The authors gratefully thank Bundesministerium für Bildung und Forschung for funding within the project VIP-project "Pyrofunk" (03SF0475A). Furthermore we thank Andreas Davids for his support concerning the confocal microscopy and the surface imaging as well as Gero Wiemann for technical support in the laboratory.

Author Contributions

Dirk Spitzner and Ute Bergmann designed the setup, Dirk Spitzner performed the experiments and analysed the data. All authors contributed to the analysis of the presented experiments and correlation

of the different means of investigations in order to reveal details of the mechanism of the icing process. Ute Bergmann coordinated the projects. Dirk Spitzner wrote the article. All authors read and approved the article.

Conflicts of Interest

The authors declare no conflict of interest.

References

1. Fillion, R.M.; Riahi, A.R.; Edrisy, A. A review of icing prevention in photovoltaic devices by surface engineering. *Renew. Sustain. Energy Rev.* **2014**, *32*, 797–809.
2. Croutch, C.K.; Hartley, R.A. Adhesion of ice to coatings and the performance of ice release coatings. *J. Coat. Technol.* **1992**, *64*, 41–53.
3. Petrenko, V.F.; Peng, S. Reduction of ice adhesion to metal by using self-assembling monolayers (SAMs). *Can. J. Phys.* **2003**, *278*, 387–393.
4. Suh, H.S.; Jang, A.R.; Suh, Y.-H.; Suslick, K.S. Porous, hollow, and ball-in-ball metal oxide microspheres: Preparation, endocytosis, cytotoxicity. *Adv. Mater.* **2006**, *18*, 1832–1837.
5. Chatterji, S. Aspects of the freezing process in a porous material-water system: Part 1. Freezing and the properties of water and ice. *Cem. Concr. Res.* **1999**, *29*, 627–630.
6. Mishchenko, L.; Hatton, B.; Bahadur, V.; Tylor, J.A.; Krupenkin, T.; Aizenberg, J. Design of ice-free nanostructured surfaces based on repulsion of impacting water droplets. *ACS Nano* **2010**, *4*, 7699–7707.
7. Jafari, R.; Menini, R.; Farzaneh, M. Superhydrophobic and icephobic surface structures prepared by RF-sputtered polytetrafluoroethylene coatings. *Appl. Surf. Sci.* **2010**, *257*, 1540–1543.
8. Auer, F.; Harenburg, J.; Roth, C. Funktionelle schichten auf metallen: Maßgeschneiderte eigenschaften durch sol-gel-technologie/functional layers on metals: Tailored properties by sol-gel-technology. *Materialwiss. Werkstofftech.* **2001**, *32*, 767–773. (In Germany)
9. Kulinich, S.A.; Farhadi, S.; Nose, K.; Du, X.W. Superhydrophobic surfaces: Are they really ice-repellent? *Langmuir* **2011**, *27*, 25–29.
10. Boinovich, L.B.; Emelyanenko, A.M.; Ivanov, V.K.; Pashinin, A.S. Durable icephobic coating for stainless steel. *ACS Appl. Mater. Interfaces* **2013**, *5*, 2549–2554.
11. Cao, L.; Jones, A.K.; Sikka, V.K.; Wu, J.; Gao, D. Anti-icing superhydrophobic coatings. *Langmuir* **2009**, *25*, 12444–12448.
12. Jung, S.; Tiwari, M.K.; Doan, N.V.; Poulikakos, D. Mechanism of supercooled droplet freezing on surfaces. *Nat. Commun.* **2012**, *3*, 615.
13. Kreider, A.; Weber, B.; Stenzel, V.; Tornow, C.; Grunwald, I. Natural frost protection—Coupling antifreeze proteins to a PU coating inhibits ice deposition. *Eur. Coat. J.* **2011**, *5*, 34–39.
14. Gibson, M.I. Slowing the growth of ice with synthetic macromolecules: Beyond antifreeze(glyco) proteins. *Polym. Chem.* **2010**, *1*, 1141–1152.
15. Chen, M.-L.; Chiou, T.-K.; Jiang, S.-T. Isolation of ice-nucleating active bacterium from mackerel and its properties. *Fish. Sci.* **2002**, *68*, 934–941.

16. Gwak, Y.; Park, J.; Kim, M.; Kim, H.S.; Kwon, J.K.; Oh, S.J.; Kim, Y.-P.; Jin, E. Creating anti-icing surfaces via the direct immobilization of antifreeze proteins on aluminium. *Sci Rep.* **2015**, *5*, doi:10.1038/srep12019.
17. Kim, P.; Wong, T.-S.; Alvarenga, J.; Kreder, M.J.; Adorno-Martinez, W.E.; Aizenberg, J. Liquid-infused nanostructured surfaces with extreme anti-ice and anti-frost performance. *ACS Nano* **2012**, *6*, 6569–6577.
18. Sidorenko, A.; Krupenkin, T.; Aizenberg, J. Controlled switching of the wetting behavior of biomimetic surfaces with hydrogel-supported nanostructures. *J. Mater. Chem.* **2008**, *18*, 3841–3846.
19. Chen, J.; Dou, R.; Cui, D.; Zhang, Q.; Zhang, Y.; Xu, F.; Zhou, X.; Wang, J.; Song, Y.; Jiang, L. Robust prototypical anti-icing coatings with a self-lubricating liquid water layer between ice and substrate. *ACS Appl. Mater. Interfaces* **2013**, *5*, 4026–4030.
20. Rykaczewski, K.; Anand, S.; Subramanyam, S.B.; Varanasi, K.K. Mechanism of frost formation on lubricant-impregnated surfaces. *Langmuir* **2013**, *29*, 5230–5238.
21. Péter, Z.; Farzaneh, M.; Kiss, L.I. Assessment of the current intensity for preventing ice accretion on overhead conductors. *IEEE Trans. Power Deliv.* **2007**, *22*, 565–574.
22. Venna, V.V.; Lin, Y.-J. Mechatronic development of self-actuating in-flight deicing structures. *IEEE-ASME Trans. Mechatron.* **2006**, *11*, 585–592.
23. Petrenko, V.F. The effect of static electric fields on ice friction. *J. Appl. Phys.* **1994**, *76*, 1216–1219.
24. Petersen, A.; Rau, G.; Glasmacher, B. Reduction of primary freeze-drying time by electric field influenced ice nucleus formation. *Heat Mass Transf.* **2006**, *42*, 929–938.
25. Ehre, D.; Lavert, E.; Lahav, M.; Lubomirsky, I. Water freezes differently on positively and negatively charged surfaces of pyroelectric materials. *Science* **2010**, *327*, 672–675.
26. Lang, S.B. Pyroelectricity: From ancient curiosity to modern imaging tool. *Phys. Today* **2005**, *58*, 31–36.
27. Poulsen, M.; Ducharme, S. Why ferroelectric polyvinylidene fluoride is special. *IEEE Trans. Dielectr. Electr. Insul.* **2010**, *17*, 1028–1035.
28. Harb, A. Energy harvesting: State-of-the-art. *Renew. Energy* **2011**, *36*, 2641–2654.
29. Navid, A.; Pilon, L. Pyroelectric energy harvesting using Olsen cycles in purified and porous poly(vinylidene fluoride-trifluoroethylene) [P(VDF-TrFE)] thin films. *Smart Mater. Struct.* **2011**, *20*, doi:10.1088/0964-1726/20/2/025012.
30. Olsen, R.B.; Bruno, D.A.; Briscoe, J.M. Cascaded pyroelectric energy converter. *Ferroelectrics* **1984**, *59*, 205–209.
31. Nordheim, D.; Hahne, S.; Ploss, B. Nonlinear dielectric properties and polarization in thin ferroelectric P(VDF-TrFE) copolymer films. *IEEE Trans. Dielectr. Electr. Insul.* **2012**, *19*, 1175–1180.